# CONTINUOUS ULTRAVIOLET ABSORPTION BY Si+(4Pe) : AN EXPLORATORY R-MATRIX CALCULATION

J. Tully

JOURNAL DE PHYSIQUE
Colloque C1, Supplément au n°3, Tome 49, Mars 1988 

# CONTINUOUS ULTRAVIOLET ABSORPTION BY $Si^+(^4P^e)$ : AN EXPLORATORY R-MATRIX CALCULATION

J.A. TULLY

*Observatoire de Nice, BP 139, F-06003 Nice Cedex, France*

RESUME: La méthode de la matrice R est utilisée pour calculer la photoionisation à partir du premier état excité $3s3p^2\ ^4P^e$ du $Si^+$. Les deux termes triplets les plus bas $3s3p\ ^3P^o$ et $3p^2\ ^3P^e$ de l'ion résiduel $Si^{++}$ sont inclus dans le calcul. Ils sont représentés par des fonctions d'onde, avec interaction de configuration, construites avec six orbitales spectroscopiques: 1s,2s,2p,3s,3p,3d. Des sections efficaces partielles et totales sont tabulées pour des énergies photoniques qui vont du seuil (705 Å) jusqu'à 2.5 Ryd (365 A). Quelques résonances dues à des états autoionisants $3p^2np$ sont délinées et portées sur des graphiques.

ABSTRACT: The R-matrix method is used to calculate photoionisation from the first excited state $3s3p^2\ ^3P^e$ of $Si^+$. The lowest two triplet terms $3s3p\ ^3P^o$ and $3p^2\ ^3P^e$ of the residual ion $Si^{++}$ are included in the calculation. They are approximated by configuration interaction wavefunctions which are constructed from six spectroscopic orbitals: 1s,2s,2p,3s,3p,3d. Partial and total cross-sections are tabulated for photon energies ranging from threshold (705 A) up to 2.5 Ryd (365 A). Some of the $3p^2np$ autoionising resonances are delineated and shown graphically.

## 1.. INTRODUCTION

The aluminium-like ion SiII possesses a rich line spectrum in the visible and ultraviolet and, owing to the high cosmic abundance of silicon, is detected in many astronomical objects. It is therefore desirable to have reliable information about the atomic properties of this ion and in particular its photoabsorption spectrum. Although two detailed calculations (1,2) have been carried out for photoionisation from the ground state, no serious attempt has yet been made to obtain the continuous absorption coefficient for excited states. Here one presents some preliminary results for photoabsorption by the metastable $^4P^e$ state.

The R-matrix approach (3) is a powerful method, based on the close coupling approximation (4), for obtaining the initial bound and final scattering states with which to compute the cross-section by means of Fermi's "Golden Rule". One has used a modified version of the well known R-matrix package RMATRX (5) to compute the cross-sections for the processes shown schematically in figure 1.

## 2. DETAILS OF THE PRESENT R-MATRIX CALCULATION

The program RMATRX requires as input wavefunctions for states of the residual ion, in this case $Si^{++}$. Since one's aim was to carry out an exploratory calculation, one chose to include only two states, viz $3s3p\ ^3P^o$ and $3p^2\ ^3P^e$. Furthermore, one represented these by fairly simple configuration interaction wavefunctions built up from orbitals 1s,2s,2p,3s,3p (6) and 3d (7). The theoretical(experimental) ionisation threshold energies are: $I(^3P^o)$ = 1.298(1.292) Ryd and $I(^3P^e)$ = 2.013(1.994) Ryd. In the third stage of RMATRX the thresholds were adjusted in the standard fashion (5) so as to agree with observation.

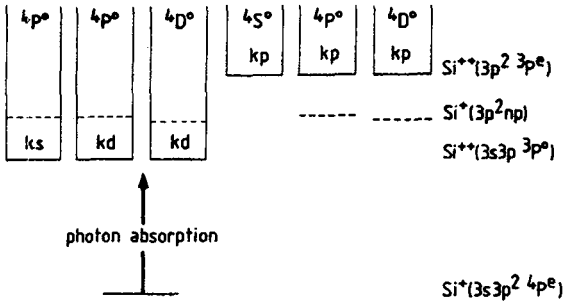


Figure 1. Schematic representation of the photoabsorption process

The R-matrix boundary was set at RA = 15.15625 a.u., which was deemed sufficiently large to ensure convergence of the dipole length and velocity matrix elements. A relatively large boundary was necessary since the version of RMATRX that one used ignores the contribution to the dipole integrals from the outer region.

One chose NRANG2 = 15 "continuum" basis orbitals to span the inner region. This enables one to use the present model for photon energies up to about 2.5 Ryd.

## 3. RESULTS

Figure 1 shows the six continuum channels based on the two lowest triplet states of $Si^{++}$. With each of these channels is associated a probability (i.e. partial cross-section) for photoionising $Si^{+}$ and leaving the residual ion in the corresponding channel state, while at the same time ejecting a photoelectron of given wave number k and orbital angular momentum l. The partial cross-sections in megabarn units (i.e. $10^{-18}$ $cm^2$) are given in Table 1 as functions of the photon energy in Rydberg units. The total cross-section, which is the quantity of interest to astronomers, is also tabulated.

The cross-sections for absorption into the kd $^4D^o$ and kd $^4P^o$ channels exhibit broad minima of the type first reported by Rudkjøbing (8) in connection with the absorption spectrum of sodium. This behaviour is caused by a change in sign of the radial matrix elements as the photon energy increases. The $^4D^o$ length cross-section, for example, drops rapidly from the value 1.14Mb at threshold (1.292 Ryd) to zero at about 1.75Ry. The $^4P^o$ cross-section vanishes at a slightly higher energy.

Between the $^3P^o$ and $^3P^e$ thresholds, i.e. for 705A > λ > 365A, the smooth variation of the cross-section is interrupted by autoionising resonances. These are caused by the $3p^2np$ terms of $Si^{+}$ which are embedded in the 3s3pks and 3s3pkd continua. The two $^4P^o$ channels interact strongly and while the resonance in ks produces an indentation in the partial cross-section, that in the kd channel gives rise to a complementary peak resulting in only a slight trough when the two are summed. Figure 2 illustrates this behaviour for the n=5 resonance which is located at $h\nu$=1.74255Ryd and has a width (FWHM) of 2.35E-03 Ryd. The first resonance in the $^4D^o$ channel occurs at about 1.52Ryd and is of the Beutler-Fano type with a negative q coefficient. The length and velocity cross-sections are compared in figure 3 and are seen to differ by a large amount. The next resonance (n=5) occurs close to where the background cross-section passes through zero and consequently its profile is approximately Lorentzian. This resonance is shown in figure 4 for the geometric mean of the length and velocity partial cross sections. A curious feature in the form of a narrow crevasse occurs on the short wavelength side of the profile and is associated with a small blip in the phase shift. The cross-section falls suddenly to zero at the point where the energy derivative of the phase shift passes through zero. One assumes that this has no physical significance and is simply due to the proximity of an R-matrix pole at 1.7376 Ryd.

Table 1. Partial and total cross sections in Mb units. + length, ++ velocity.

| hν/Ryd | ks $^4P^o$ | kd $^4P^o$ | kd $^4D^o$ | kp $^4S^o$ | kp $^4P^o$ | kp $^4D^o$ | Total |
|---|---|---|---|---|---|---|---|
| 1.2924 | 0.794+ | 0.436 | 1.140 | | | | 2.37 |
| | 0.800++ | 0.335 | 1.060 | | | | 2.20 |
| 1.40 | 0.692 | 0.251 | 0.525 | | | | 1.47 |
| | 0.698 | 0.169 | 0.460 | | | | 1.33 |
| 1.50 | 0.603 | 0.153 | 0.131 | | | | 0.88 |
| | 0.634 | 0.071 | 0.045 | | | | 0.75 |
| 1.60 | 0.556 | 0.061 | 0.090 | | | | 0.70 |
| | 0.538 | 0.045 | 0.100 | | | | 0.68 |
| 1.70 | 0.491 | 0.027 | 0.004 | | | | 0.52 |
| | 0.500 | 0.010 | 0.003 | | | | 0.51 |
| 1.80 | 0.440 | 0.007 | 0.001 | | | | 0.44 |
| | 0.440 | 0.001 | 0.000 | | | | 0.44 |
| 2.00 | 0.356 | 0.001 | 0.042 | 0.006 | 0.008 | 0.061 | 0.47 |
| | 0.352 | 0.004 | 0.037 | 0.005 | 0.033 | 0.099 | 0.53 |
| 2.10 | 0.326 | 0.003 | 0.073 | 0.008 | 0.010 | 0.074 | 0.49 |
| | 0.321 | 0.008 | 0.066 | 0.007 | 0.036 | 0.112 | 0.55 |
| 2.20 | 0.303 | 0.007 | 0.088 | 0.010 | 0.012 | 0.065 | 0.48 |
| | 0.292 | 0.010 | 0.077 | 0.008 | 0.026 | 0.094 | 0.50 |
| 2.30 | 0.281 | 0.013 | 0.115 | 0.012 | 0.015 | 0.075 | 0.51 |
| | 0.271 | 0.018 | 0.101 | 0.010 | 0.036 | 0.102 | 0.53 |
| 2.40 | 0.261 | 0.019 | 0.141 | 0.009 | 0.017 | 0.079 | 0.52 |
| | 0.250 | 0.023 | 0.122 | 0.010 | 0.038 | 0.105 | 0.54 |
| 2.50 | 0.242 | 0.025 | 0.165 | 0.013 | 0.019 | 0.081 | 0.54 |
| | 0.230 | 0.029 | 0.141 | 0.012 | 0.038 | 0.105 | 0.55 |

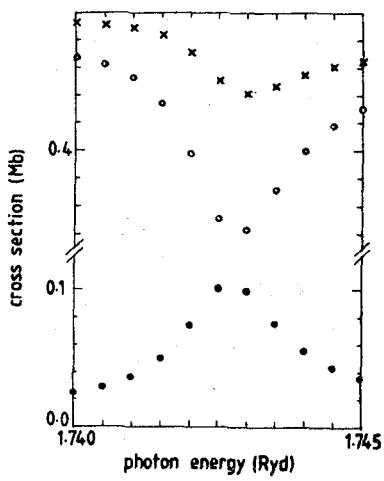


Figure 2. Profiles of the length partial cross sections for the $3p^2 5p\ ^4P^o$ resonance. ks channel (o), kd channel (•), sum (x).

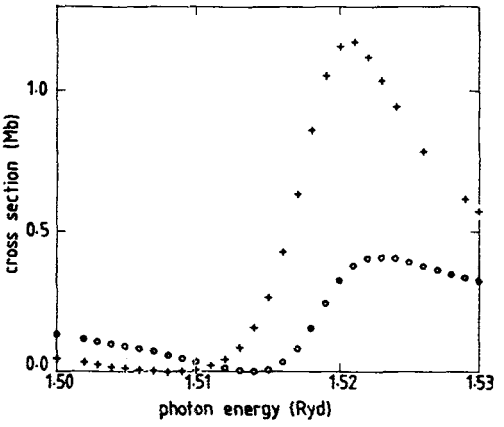


Figure 3. Length (o) and velocity (+) partial cross sections near the $3p^2 4p\ ^4p^o$ resonance.

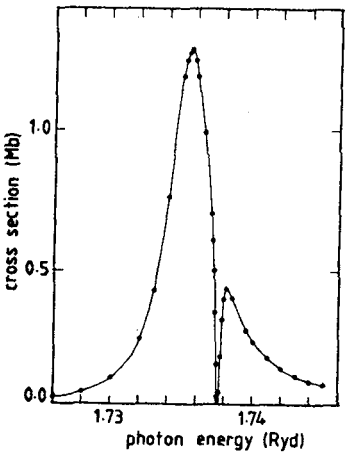


Figure 4. Profile of the geometric mean cross section for the $3p^2 5p\ ^4p^o$ resonance.

## 4. A NOTE ON THE OUTER REGION SOLUTIONS

The inner and outer region solutions are matched on the R-matrix boundary. In the present case one assumed that the value of RA was sufficiently large to justify the use of a Coulomb potential in the outer region. The asymptotic solutions were therefore obtained by interfacing the third stage of RMATRX to a program for generating Coulomb functions. The validity of this approximation was tested by comparing some of the present results with those obtained by interfacing RMATRX to the AYSPCK (9) package. In some cases differences of more than a few percent were encountered and so further work is clearly required for this photoionisation process in order to have complete confidence in the results.

A final note concerning the use of ASYPCK (9) is of relevance here. It is important to take account of the charge dependent normalisation used by Crees for the radial continuum functions (c.f. (9), section 2.4.1). These oscillate asymptotically with amplitude $\sqrt{(z/k)}$, where z is the charge of the residual ion. This fact was overlooked in the previous R-matrix calculation devoted to SiII and consequently the cross-sections given in reference (2) should be divided by 2 (the charge of $Si^{++}$).

## ACKNOWLEDGEMENTS

I thank Dr. K.A. Berrington for providing me with copies of the programs used in the present study and also for a clarifying discussion. Dr. C.J. Zeippen helped in localising the z factor discrepancy associated with the use of RMATRX+ASYPCK.

## REFERENCES

1. Daum G.R. and Kelly H.P. 1976 Phys.Rev. A13, 715.
2. Taylor K.T., Zeippen C.J. and Le Dourneuf M. 1984 J.Phys.B 17, L157.
3. Burke P.G. and Taylor K.T. 1975 J.Phys.B 8, 2620.
4. Burke P.G. and Seaton M.J. 1971 Methods Comput. Phys. 10, 1.
5. Berrington K.A., Burke P.G., Le Dourneuf M., Robb W.D., Taylor K.T. and Vo Ky Lan. 1978 Comput. Phys. Commun. 14, 367.
6. Clementi E. and Roetti C. 1974 Atomic Data and Nucl. Data Tables 14, 177.
7. Baluja K.L. and Hibbert A. 1980 J.Phys.B 13, L327.
8. Rudkjøbing M. 1940 Publ. Kbh. Obs. 18, 1.
9. Crees M.A. 1980 Comput. Phys. Commun. 19, 103.